Detent Force Minimization of a Tubular Flux-Switching Permanent Magnet Motor Using Un-Equal Width Stator Slots Based on Taguchi Method

Shaopeng Wang, Youhua Wang, Chengcheng Liu, Gang Lei, Jianguo Zhu, and Youguang Guo

***Abstract*—The detent force caused by the cogging effect and end effect will seriously affect the operation of a tubular flux-switching permanent magnet motor (TFSPMM). This paper proposes a method to weaken the end effect and minimize the detent force and force ripple of a TFSPMM using un-equal width stator slots. To overcome the problem of excessive calculation, the Taguchi method is performed to find the optimal combination of stators with unequal slot width. The proposed method can significantly decrease the detent force and force ripple and keep the thrust force basically unchanged. The permanent magnet flux linkage, detent force and electromagnetic force are calculated by the two dimensional (2D) finite element method (FEM).**

***Index Terms*—Detent force, tubular flux-switching permanent magnet motor (TFSPMM), unequal width stator slots, Taguchi method, 2D finite element method (FEM).**

I. Introduction

TUBULAR flux-switching permanent magnet motor (TFSPMM) is a special kind of permanent magnet machine with the permanent magnet (PM) installed on the stator side and there is no winding or PMs on the mover side[1-2]. Compared with other linear machines, TFSPMM's tubular structure avoids the motor thrust fluctuation caused by transverse side effect. However, the TFSPMM is still opened at two ends, which will destroy the integrity of the magnetic circuit. The end effect can bring the TFSPMM with higher detent force, higher force ripple and un-symmetry of the PM flux linkage especially for phase A and phase B since they have end winding, and these problems will bring difficulties to the stable output and control of the motor[3-6]. Based on these situations, a new method of un-equal width stator slots design is proposed to reduce the end effect. On the premise of not changing the volume of the motor, the end effect of the motor can be weakened by coordinating the axial length of the stator slot and the axial length of the adjacent PMs, so as to improve the symmetry of the three-phase PM flux linkage and reduce the detent force. The calculation results are mainly based on the analysis of the average value and peak-to-peak value of the A-phase PM flux linkage and detent force, electromagnetic force, because the A-phase and B-phase windings are symmetric in position and contain the end windings.

To reduce the calculation time, the Taguchi method is adopted for the design process. It is a local optimization method proposed by Dr. Taguchi from Japan based on orthogonal test and signal to noise ratio technology[7-8]. Compared with other local optimization method, the Taguchi method can optimize design for multiple objectives, and analyze the optimal combination of design parameters in the multi-objective optimal design with the minimum number of experiments by establishing the orthogonal table of experiments[9-10]. For the design optimization of this machine, average value and peak-to-peak value of PM flux linkage of A phase and detent force will be used as optimization targets, the width of slot1, slot2 and slot3 are used as control factor and the level number of them are 5.

II. Topology of TFSPMM and Main Parameters

Fig.1 shows the main topology and main design parameters of TFSPMM. The permanent magnets (PMs) in TFSPMM are located on the short primary stator side and they are magnetized along the axial direction. Adjacent PMs are magnetized along the opposite directions, and all the PMs are sandwiched between the U-shaped stator cores. The used winding is the global ring winding and it is located on the inner space of U shaped stator cores. In TFSPMM, there is no winding or PM

This work was supported in part by the Natural Science Foundation of Hebei Province under Project E2019202220, in part by National Natural Science Foundation of China under Project 51877065, in part by Hebei Province Education Department Youth Talent Leading Project under grant BJ2018037, and in part by the State Key Laboratory of Reliability and Intelligence of Electrical Equipment under Grant EERIKF2018005.

Shaopeng Wang, Youhua Wang and Chengcheng Liu are with State Key Laboratory of Reliability and Intelligence of Electrical Equipment, Hebei University of Technology and Key Laboratory of Electromagnetic Field and Electrical Apparatus Reliability of Hebei Province, Hebei University of Technology, Tianjin, 300130, China (2016020@hebut.edu.cn, 522396000@qq.com, wangyi@hebut.edu.cn).

Gang Lei, and Youguang Guo are with the School of Electrical and Data Engineering, University of Technology Sydney, NSW 2007, Australia, (gang.lei@uts.edu.au, youguang.guo@uts.edu.au)

Jianguo Zhu is with school of electrical and information engineering, University of Sydney, NSW 2007, Australia, (jianguo.zhu@sydney.edu.au)

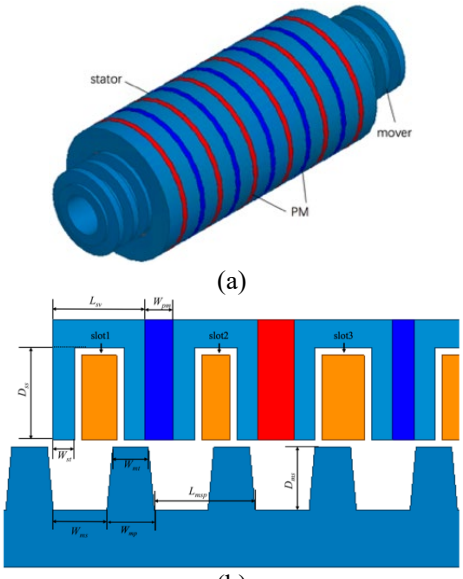

Fig. 1. Main topology and parameters of the TFSPMM. (a) topology of the 3-D traditional TFSPMM, (b) parameters of the traditional TFSPMM.

on the long mover side, thus the material cost can be kept very low and the mechanical robustness can be guaranteed. To reduce the calculation load, the main electromagnetic parameters and performance of TFSPMM are obtained based on the 2D finite element method (FEM), and the model shown in Fig.1(b) is built around Z-axis, which can be considered as rotational symmetry around the Z-axis. The parameters shown in Table I are the initial design for the optimization. The target of the machine is used for the verification of a suspension system, the rated power of 1000 W and the outer diameter of 100 mm and the effective length of 200 mm needs to be met. These are the main constraints of this machine, and as for the mechanical and electromagnetic constraints, these machine is design with the water cooling and as the SMC material is used for the part of stator core, the minimum length of the part with SMC needs to be higher than 3 mm. As for the electromagnetic constraints the maximum current density of 15A/mm^2 is determined.

TABLE I MAIN DIMENSIONS OF PROPOSED TFSPMM

Parameters	Symbol	Value	Unit
Stator inner radius	R_{si}	33	mm
Stator outer radius	R_{so}	50	mm
Stator yoke length	L_{sy}	13	mm
Stator slot depth	D_{ss}	7	mm
Stator tooth width	W_{st}	3	mm
PM width	W_{pm}	4	mm
Effective axial length	L_{ea}	200	mm
Air gap length	L_{ag}	1	mm
Shaft radius	R_{shaft}	15	mm
Mover outer radius	R_{mo}	32	mm
Mover slot depth	D_{ms}	9	mm
Mover slot width	W_{ms}	200/14-6.68	mm
Mover teeth width	W_{mt}	5	mm
Mover slot pitch length	L_{msp}	200/14	mm

III. DETENT FORCE MINIMIZATION OF TFSPMM BY UNEQUAL WIDTH STATOR SLOTS BASED ON TAGUCHI METHOD

In the previous calculation, three stators at the end were selected as optimization parameters, and the performance of the motor with the variation of their slot width have been obtained. The width of slot1, slot2 and slot3 varies from 12mm to 14mm, with the step size of 1. A total number of 27 different combinations have been produced, and the best result shown in Fig. 2 can be obtained.

The peak-to-peak value of detent force has been reduced from 178 N to 135 N. And the average value of thrust force has been reduced from 519 N to 492 N. However, the force ripple of the initial design is about 0.407 while that for the optimized design is about 0.265. Although the thrust decreased by 4.9%, the peak-to-peak value of thrust is decreased by 38.0% from 221.7 N to 131.2 N. And the percentage force ripple is defined as

$$F_{rip} = \frac{F_{max} - F_{min}}{F_{ave}} \quad (1)$$

where F_{max}, F_{min}, and F_{ave} are the maximum, minimum, and

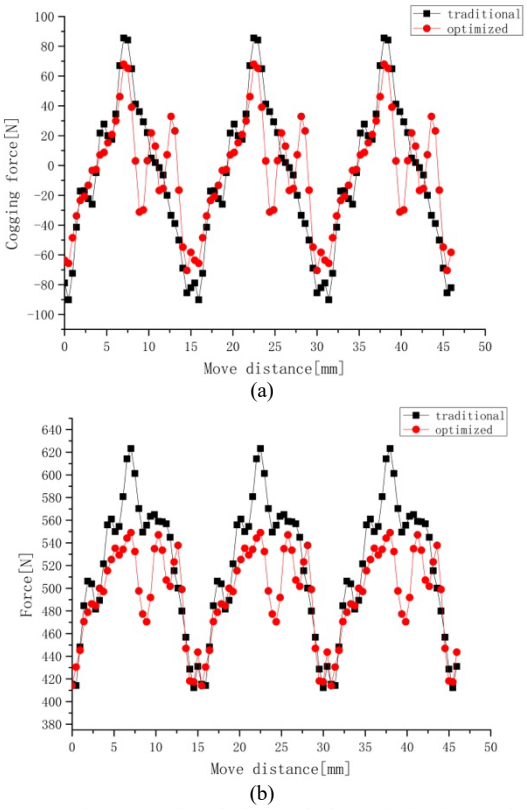

Fig. 2. TFSPMM force waveform before and after optimization (a) detent force of the TFSPMM, (b) force of the TFSPMM.

average force, respectively.

However, when the number of parameter changes increases, as shown in Table II, the number of parameter changes is 5, which produces a total 125(5*5*5) different combinations. It will take a very large amount of computer resources and a very long time to complete the calculation by using software.

TABLE II OPTIMIZATION VARIABLES AND VALUE LEVELS OF TFSPMM

Control factors	Slot1/mm	Slot2/mm	Slot3/mm
Level 1	12	12	12
Level 2	12.5	12.5	12.5
Level 3	13	13	13
Level 4	13.5	13.5	13.5
Level 5	14	14	14

By using the Taguchi method, only 25(5*5) different combinations need to be calculated, which saves computer resources, reduces computing time and improves computing efficiency. Based on the number of selected parameters and the number of levels, the orthogonal table can be established and represented by $L_n(t^c)$, where L is the code of orthogonal table, n the number of experiments, t the number of levels, and c the number of columns, that is, the number of parameters that can be arranged the most. The orthogonal table shown in Table III, includes 25 different levels of combinations and their corresponding electromagnetic performances. As the value of stator slot width varies from 12mm to 14mm, and the step length is 0.5mm, as shown in Table II, it has five levels, and the level number 5 is the case where the slot width is equal to 14mm.

TABLE III EXPERIMENT MATRIX AND FE RESULT

No	Control factors			Ψ_A/mWb	Ψ_{PP}/mWb	F_{PP}/N
	Slot1	Slot2	Slot3			
1	1	1	1	-1.4	2.8	146
2	1	2	2	-1.4	2.9	208
3	1	3	3	-1.3	3	246
4	1	4	4	-1.2	3	254
5	1	5	5	-1.1	2.9	252
6	2	1	2	-1.1	2.8	96
7	2	2	3	-1	2.9	182
8	2	3	4	-0.9	3	249
9	2	4	5	-0.8	2.9	296
10	2	5	1	-2.2	2.9	114
11	3	1	3	-0.6	2.8	67
12	3	2	4	-0.5	2.9	173
13	3	3	5	-0.4	2.9	273
14	3	4	1	-1.8	2.9	149
15	3	5	2	-1.8	2.9	87
16	4	1	4	-0.2	2.8	90
17	4	2	5	0	2.8	183
18	4	3	1	-1.4	2.8	143
19	4	4	2	-1.4	2.9	115
20	4	5	3	-1.4	2.9	82
21	5	1	5	0.4	2.7	134
22	5	2	1	-1	2.7	86
23	5	3	2	-1	2.8	89
24	5	4	3	-1	2.9	80
25	5	5	4	-0.9	2.8	76

The average value, peak-to-peak value of PM flux linkage, and peak-to-peak value of detent force are used as optimization targets in the Taguchi method and represented by Ψ_A, Ψ_{PP} and F_{PP}. The results of this three optimization parameters are obtained by calculating 25 combinations in Table III with finite element software.

According to the Taguchi method, the average value of each parameter in 25 groups of data is calculated by the formula (2), and the results are shown in Table IV.

$$m=\frac{1}{n}\sum_{i=1}^{n}m_i \tag{2}$$

TABLE IV AVERAGE VALUES OF EXPERIMENTS

Parameters	Ψ_A/mWb	Ψ_{PP}/mWb	F_{PP}/N
Average	-1.016	2.864	158

where m is the average value of all experimental results of one parameter in Table III, n the number of experiments, m_i the value of experimental result of one parameter in its i^{th} experiment. The average value of an optimization parameter for a certain control factor at a certain level can be obtained. For example, the following formula (3) calculates the average value of the average value of the PM flux linkage when slot1 is at level 1. The calculation results are shown in Table V.

$$m_{\psi_A}(slot_1)=\frac{1}{5}(\psi_{A1}+\psi_{A2}+\psi_{A3}+\psi_{A4}+\psi_{A5}) \tag{3}$$

Ψ_{A1}~ Ψ_{A5} respectively represents the average values of Ψ_A of 5 experiments when the level of stator slot1 is 1.

To know the effect of the optimization parameters on the target more directly, the data in Table V is made into the broken line diagram as shown in Fig. 3. As shown, with the increase of the width of stator slot1 and slot3, the average value of PM flux linkage decreases gradually. On the contrary, the average value of the PM flux linkage increases gradually with the increase of the width of stator slot2. For the peak-to-peak value of PM flux linkage shown in Fig. 3(b), the parameter changes have little influence on it. As for the peak-to-peak value of detent force shown in Fig. 3(c), it decreases with the increase of width of stator slot1, and when the width of slot2 and slot3 increases, it shows the maximum and minimum value respectively.

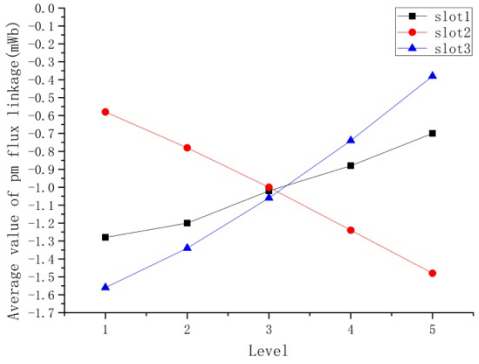

(a)

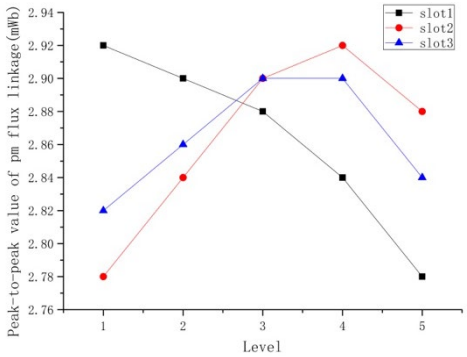

(b)

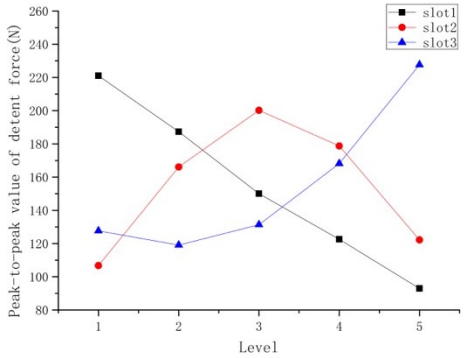

(c)

Fig. 3. The electromagnetic performance of each parameter at different levels, (a) the average value of the pm flux linkage at different levels of each parameter, (b) the peak-to-peak value of the pm flux linkage at different levels of each parameter, (c) the peak-to-peak value of the detent force at different levels of each parameter.

As tabulated in Table V, the level combination of control factors can be obtained directly which respectively minimize the average value of PM flux linkage, maximize the peak-to-peak value of PM flux linkage and minimize the peak-to-peak value of detent force. However, it is necessary to consider the variation of multiple parameters at the same time in motor de sign. In order to give consideration to all optimization parameters, it is necessary to balance the proportion of each of them so as to obtain the optimal result.

TABLE V AVERAGE VALUES OF PERFORMANCE INDEXES FOR PARAMETERS AT EACH LEVEL

Control factors	Level	Ψ_A/mWb	Ψ_{PP}/mWb	F_{PP}/N
Slot1	1	-1.28	2.92	221
	2	-1.2	2.9	187
	3	-1.02	2.88	150
	4	-0.88	2.84	123
	5	-0.7	2.78	93
Slot2	1	-0.58	2.78	107
	2	-0.78	2.84	166
	3	-1	2.9	200
	4	-1.24	2.92	179
	5	-1.48	2.88	122
Slot3	1	-1.56	2.82	128
	2	-1.34	2.86	119
	3	-1.06	2.9	131
	4	-0.74	2.9	168
	5	-0.38	2.84	228

According to the average values of the obtained parameters in all experiments and at each level, the proportion of the influence of each control factor on the optimization parameter can be obtained by solving the variance. The results can be calculated by the following formula (4) and (5),

$$\sigma^2=\frac{1}{N}\sum_{i=1}^{N}(X_i-\mu) \tag{4}$$

$$\sigma^2=\frac{1}{5}\sum_{i=1}^{5}\left[m_n(S_i)-m(S)\right]^2 \tag{5}$$

where σ^2 is the variance, N the number of level (5 in this paper), X the variable ($m_n(S_i)$in this paper), μ the population average ($m(S)$in this paper).

As shown in Table VI, the larger the percentage of variance, the greater the effect of the slot structure on the corresponding performance. The change of slot1 has a great influence on the peak-to-peak value of detent force, meanwhile, slot3 has a great influence on the average value of PM flux linkage. According to the selection principle, slot 1 has the greatest influence on the peak-to-peak value of positioning force. Therefore, the level of slot 1 with the minimum positioning force is selected in table 5, which is level 5. Similarly, the levels of slot 2 and slot 3 can also be determined by this method. The combination level of the initially selected control factors is Slot1(5), Slot2(4), Slot3(5). It was found that the result of Slot1(5), Slot2(2), Slot3(4) was better when the neighboring combination was calculated, so the final result was determined to be Slot1(5), Slot2(2), Slot3(4). Since the values of Ψ_A and Ψ_{PP} in the selected performance are both very small and close, more compromises are made to the combination of small peak-to-peak values of the detent force in the end. Topology of the 2-D traditional TFSPMM and optimized TFSPMM are shown in Fig. 4.

TABLE VI VARIANCE AND RATIO OF PERFORMANCE INDEXES FOR PARAMETERS AT 5 LEVELS

Parameters	Ψ_A/Wb		Ψ_{PP}/Wb		F_{PP}/N	
	σ^2x10^8	ratio	σ^2x10^9	ratio	σ^2	ratio
Slot1	4.44	13.7%	2.46	41.4%	2067	42.1%
Slot2	10.23	31.6%	2.46	41.4%	1227	25%
Slot3	17.67	54.6%	1.02	17.2%	1610	32.8%

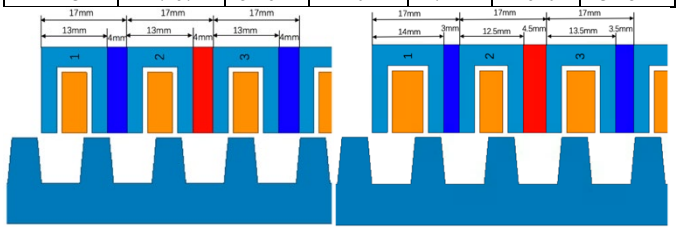

(a) (b)

Fig. 4. Topology of the 2-D traditional TFSPMM and optimized TFSPMM. (a) traditional TFSPMM, (b) optimized TFSPMM.

In the new structure, the volume of silicon steel is increased and the volume of PMs is reduced, which also reduces the material cost of the motor.

Fig. 5 shows the comparison of A phase PM flux linkage between the initial design and the second optimized design. It can be found that the symmetry of PM flux linkage has been improved after the optimization, and the sinusoidal property is not affected. The peak-to-peak value of the PM flux linkage decreased from 2.93mWb to 2.80mWb, with a decrease rate of 4.4%. Optimized TFSPMM has the un-equal width stator slots structure which makes the flux of the end side winding much closer to that the middle side winding.

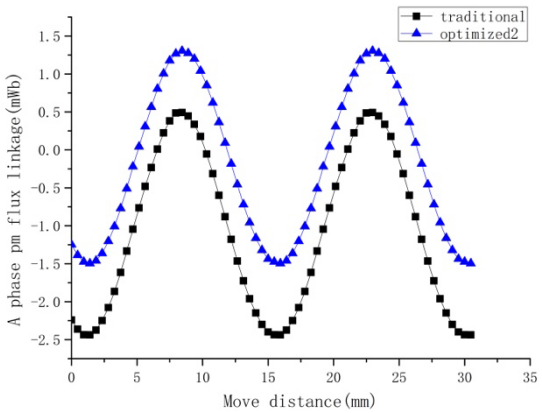

Fig. 5. PM flux linkage of the traditional TFSPMM and optimized TFSPMM.

Fig. 6 and Fig. 7 show the detent force and thrust force comparison among the initial design and two optimized designs. It can be seen that the peak-to-peak value of the detent force and thrust force of the TFSPMM with the second optimized design is much lower than that with initial design and the first optimized design at the same current density. The peak-to-peak

value of detent force has been reduced from 180 N at the beginning to 135 N under the first optimization design, and then to 68 N under the second optimization design.

As well as the average value of thrust was reduced from 520 to 492 and then increased to 511 N. However, the force ripple of the initial design is about 0.421, the first optimized design is 0.265, while that for the second optimized design is about 0.164. Although the thrust decreased by 1.7% from 520 N to 511 N, the peak-to-peak value of thrust decreased by 61.7% from 218.7 N to 83.8 N. It is found that un-equal width stator slots can be an effective way to reduce the detent force and force ripple. Moreover, Taguchi method is more efficient than the first optimization method. For all applications, the low force ripple and quick response are very important, thus the optimized un-equal width stator slots design can bring the TFSPMM with better performance.

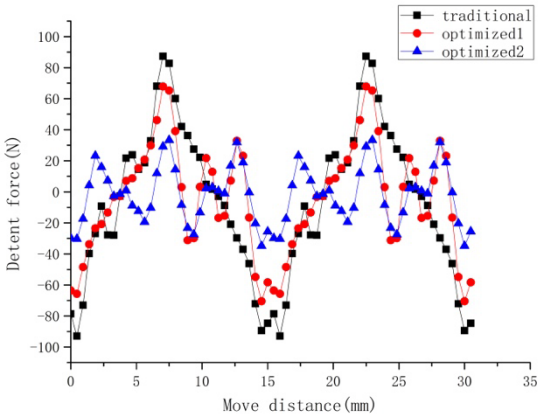

Fig. 6. Detent force of the traditional TFSPMM and optimized TFSPMMs.

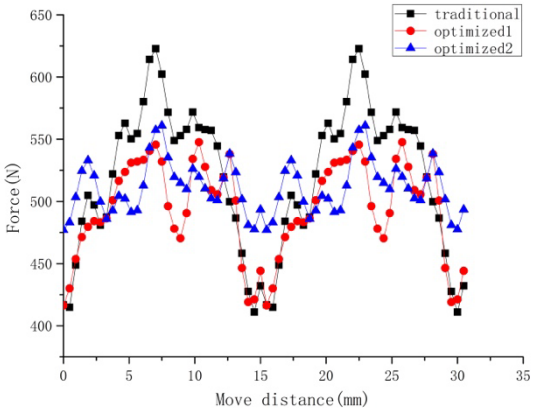

Fig. 7. Force of the traditional TFSPMM and optimized TFSPMMs.

IV. Conclusion

To reduce the end effect impact of TFSPMM, the un-equal width stator slots is proposed on the premise of not changing the volume of machine. Specifically, the detent force and force ripple are reduced and the symmetry of the PM flux linkage is improved by using the un-equal width stator slots design. To reduce the calculation time, Taguchi method is adopted to optimize three stator slots at the end of the TFSPMM, aiming at obtaining minimum average value of PM flux linkage, maximum peak-to-peak value of PM flux linkage and minimum detent force. The new structure provides a effective way to reduce the detent force and force ripple of the TFSPMM and the Taguchi method is effective in optimization design.

References

[1] B. Zhang, M. Cheng, J, Wang, and S. Zhu, "Optimization and analysis of a yokeless linear flux switching permanent magnet machine with high thrust density," *IEEE Trans. Magn*., vol. 51, no. 11, pp. 8204804, Nov.2015.

[2] Chengcheng Liu, Shaopeng Wang, Youhua Wang, Gang Lei, Youguang Guo, Jianguo Zhu, "Development of a new flux switching transverse flux machine with the ability of linear motion," *CES Transactions on Electrical Machines and Systems*., vol. 2, no. 4, pp. 384-391, Dec. 2018.

[3] Liang Yan, Wei Li, Zongxia Jiao, Chin-Yin Chen, and Ming Chen, "Design and Modeling of Three-phase Tubular Linear Flux-Switching Permanent Magnet Machine," Proceedings of 2014 *IEEE Chinese Guidance, Navigation and Control Conference*, August 8-10, 2014, Yantai, China

[4] N. Bianchi, S. Bolognani, D. Corte, and F. Tonel, "Tubular linear permanent magnet machines: An overall comparison," *IEEE Trans. Ind. Appl*., vol. 39, no. 2, pp. 466–475, 2003.

[5] Wang Canfei, Shen Jianxin, W. Yu, et al. "A New Method for Reduction of Detent Force in Permanent Magnet Flux-Switching Linear Machines," *IEEE Trans. Magn*., vol. 45, no. 6, pp. 2843-2846, 2009.

[6] Chengcheng Liu, Xue Li, Gang Lei, Bo Ma, Long Chen, Youhua Wang, Jianguo Zhu, "Performance Evaluation of an Axial Flux Claw Pole Machine With Soft Magnetic Composite Cores," *IEEE Trans Appl Supercond.*, vol. 28, no. 3, pp. 1890–1893, 2000.

[7] Sung - II K,Ji-Young L,Young-Kyoun K,et al. Optimization for reduction of torque ripple in interior permanent magnet motor by using the Taguchi method [J]. *IEEE Transactions on Magnetics*., 2005, 41 (5): 1796-1799.

[8] J. Song, F. Dong, J. Zhao, S. Lu, S. Dou, and H. Wang, "Optimal design of permanent magnet linear synchronous motors based on Taguchi method," *IET Elect. Power Appl.*, vol. 11, no. 1, pp. 41–48, 2017.

[9] G. Lei, C. Liu, Y. Li, D. Chen, Y. Guo, J. Zhu, "Robust Design Optimization of a High-Temperature Superconducting Linear Synchronous Motor Based on Taguchi Method," *IEEE Trans Appl Supercond.*,vol. 29, no. 2, Article#3600206, March 2019.

[10] G. Lei, C. Liu, J. Zhu, and Y. Guo, "Techniques for multilevel design optimization of permanent magnet motors," *IEEE Trans. Energy Convers.*,vol. 30, no. 4, pp. 1574-1584, Dec. 2015.